



Comparative studies on performance of solar towers with variable scale ratios

Rajamurugu Natarajan¹ · Venkatesan Jayaraman² · Ravishankar Sathyamurthy³

Received: 18 August 2021 / Accepted: 2 February 2022 / Published online: 11 February 2022
© The Author(s), under exclusive licence to Springer-Verlag GmbH Germany, part of Springer Nature 2022

Abstract

Improvements in the geometry of solar towers are explained in this study. Both computational and experimental studies are carried out. Three different solar towers of 1:60, 1:70, and 1:122 scale ratios are taken for the study. All the studies are carried out in an open atmosphere, where a hot wire anemometer is used to measure the peak velocity at the collector–tower junction. The collector geometry is kept flat, inclined, and semi-divergent. The tower geometry is modified from the straight tower into semi-divergent and fully divergent towers. The fully divergent tower with a semi-convergent collector achieves the highest power output among the other two models. The area convergence is the prime factor for an increase in peak velocity. The divergent tower with a semi-convergent collector achieves 54% more power output than a cylindrical tower with a flat collector.

Keywords Solar tower · Experiment measurements · CFD

Nomenclature

α	coefficient of absorptivity
θ	ambient condition
$\eta_{\text{collector}}$	efficiency of the collector
η_{turbine}	efficiency of the turbine
η_{tower}	efficiency of the tower
ΔP	pressure difference for driving potential
ε	coefficient of emissivity
Q_{solar}	solar irradiance in W/m^2
ρ	density in kg/m^3
C_p	specific heat capacity at constant pressure
β	thermal expansion rate
T_0	reference buoyancy temperature
STPP	solar tower power plant

Introduction

Most research papers investigated the effect of inclined collectors or modifying tower shapes individually on the performance of the solar tower power plant (STPP). In this work, the effect of the inclined collector with a divergent tower is studied by carrying out an experimental and computational study. Furthermore, both computational and experimental results of the modified STPP and the conventional STPP were compared. For both cases, the Manzanares pilot plant was kept as the base model. A new type of STPP is suggested at the end of the study; the concept is validated through experimental study.

An STPP is a thermal–mechanical device, where solar energy is converted into thermal energy. Solar energy resources are clean, free, and inexhaustible. The solar tower power plant operates on the principle that air gets heated up under a large greenhouse-like collector; the warm air enters into the tower due to the buoyancy effect and runs the turbine at the base generating electricity. The main parts of an STPP are namely the collector, tower, and turbine. The mathematical model described by Prof. Schlaich (2000) states the expression for the power output of the STPP as

$$P = Q_{\text{solar}} \eta_{\text{collector}} \eta_{\text{turbine}} \eta_{\text{tower}} \quad (1)$$

Responsible Editor: Philippe Garrigues

✉ Rajamurugu Natarajan
rmnshivsai1210@gmail.com

¹ Department of Aeronautical Engineering, Bharath Institute of Science and Research, BIHER, Chennai, India

² Department of Automobile Engineering, Sri Venkateswara College of Engineering, Sriperumbudur, India

³ Department of Mechanical Engineering, KPR Institute of Engineering, Tamil Nadu, Arasur, Coimbatore 641407, India

The total efficiency of the plant depends on the efficiencies of the individual components. The solar energy which is input for the plant depends on the area of the collector; the efficiency of the tower is dependent on its height. The air beneath the collector gets heated and increased due to the buoyancy effect (Schlaich et al. 2000); hence, a pressure difference arises and leads to flow into the tower.

$$P = \Delta PV_{\max}^2 A_{\text{collector}} \quad (2)$$

Due to buoyancy change in the warm air, the pressure difference leads to flow into the tower theoretically; the pressure difference is converted into velocity in the tower. The efficiency of the tower is expressed as

$$\eta_{\text{tower}} = \frac{gh}{C_p T_o} \quad (3)$$

Mathematical Eqs. 1, 2, and 3 impose three important phenomena. The efficiency is constrained to the tower's height, collector area, and pressure drop in the turbine. The conventional towers adopt long, tall, and straight circular geometry towers (Bilgen et al. 2005, Cao et al. 2013), and also flat circular collectors (Schlaich et al. 2000). The less power output is the main concern that prevailed in those studies. To enhance the power output, geometrical modifications to the STPP are recommended in the recent studies (Koonsriuk et al. 2014; Gholamalizadeh and Kim 2016; Patel et al. 2014; Hu et al. 2017). For the present study, the tower shape has been taken as the research area. Several researchers introduced the concept of a sloped collector instead of a flat collector (Fei cao et al. 2013; Gholamalizadeh and Kim 2016; Takmil Sakir et al. 2014; Morrison et al. 2017; Rajamurugu et al. 2021). Koonsriuk et al. (2013) investigated the STPP with an area ratio (ratio of the inlet to the outlet of collector and chimney geometries) of 0.15 to 16.0, proving that divergent towers showed better results compared with cylindrical towers. Gholamalizadeh et al. (2016) investigated with an area ratio of 0.25 to 2.25, Patel et al. (2014) investigated by changing the divergent angle from 0 to 3°, and Okade et al. (2015) considered a divergent angle of 4°. This research explained that the driving factor for divergent tower performance is the area ratio and divergent angle. Hu et al. (2017) conducted a study on diffuser-type towers with three different combinations and found that the divergent diffuser solar tower was efficient and elaborated two controlling parameters, namely area ratios of both the collector and chimney along with the divergent angle of the chimney. The incidence of sunrays with a greater angle reduces the energy absorption on the absorbing surface. To increase to a higher mass flow rate, a sloped solar tower could be a feasible option (Roozbeh Sangi 2012). The sloped collector will improve the absorbing capacity of the collector surface; furthermore, this acts as a natural tower, and therefore, the dependency on the tower height for overall efficiency may be alleviated. This paper discusses the combined effect of the divergent diffuser and sloped collector on the power output of the plant. Most of the

research (Gholamalizadeh et al. 2016; Hu et al. 2017; Koonsriuk et al. 2013; Takmil Sakir 2014; Morrison et al. 2017; Rajamurugu et al. 2021) treats the effect of a variable geometry diffuser and a sloped collector as separate entities but not much attention is given to the dual combination of a sloped collector and a curved diffuser either as computation/experimental studies. The investigation of the effect of tower geometry with an inclined collector is tried with computational studies (Koonsriuk et al. 2013; Morrison et al. 2017). Also, an attempt is made in this study to change the collector angle to increase the absorption of solar energy. The cylindrical tower is modified based on the simulation results. Three models are taken for this study:

- Model 1: straight cylindrical tower with a flat collector
- Model 2: top divergent tower with an inclined collector
- Model 3: fully divergent tower with a semi-divergent collector

All the models are experimentally studied in an open environment. Figure 1 shows the research flow.

Computational analysis of STPP

In this study, only the steady-state flow in the solar tower is simulated under the following assumptions. To formulate this model, the following assumptions were made:

- i. The fluid is Newtonian and incompressible.
- ii. The flow is steady, three-dimensional, and turbulent.
- iii. The flow field is axisymmetric.
- iv. The pressure drop in the collector region is not considered.
- v. The temperature difference across the tower outlet and inlet is small; hence, the heat transfer equation is considered only for the collector.
- vi. The transient changes in the values of solar radiation are not accounted for.
- vii. There is no-slip condition near the wall surface.
- viii. The Boussinesq approximation is assumed to be valid.

The governing equations of the present numerical model are as follows:

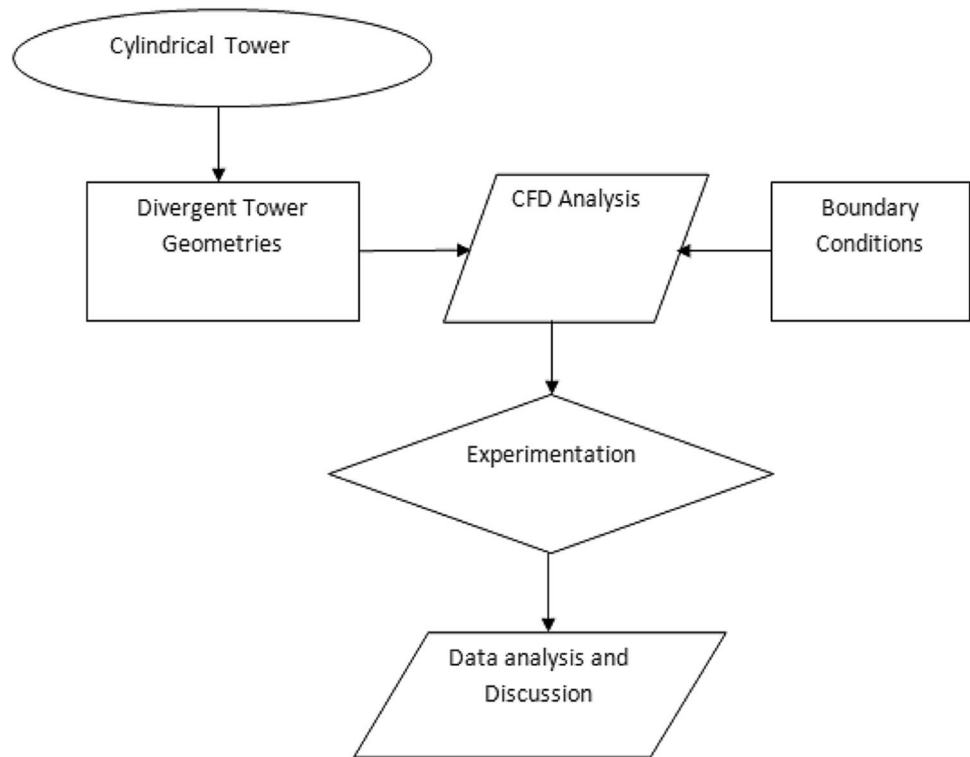
Continuity equation:

$$\frac{\partial(\rho u)}{\partial x} + \frac{1}{r} \frac{\partial(r\rho v)}{\partial r} = 0 \quad (4)$$

Momentum equations:

$$\begin{aligned} \frac{\partial(\rho uu)}{\partial x} + \frac{1}{r} \frac{\partial(r\rho uv)}{\partial r} = & -\frac{\partial p}{\partial x} + (\rho - \rho_0) g + 2 \frac{\partial}{\partial x} \left[(\mu + \mu_t) \frac{\partial u}{\partial x} \right] \\ & + \frac{1}{r} \frac{\partial}{\partial r} \left[(\mu + \mu_t) r \left(\frac{\partial u}{\partial x} + \frac{\partial v}{\partial r} \right) \right] \end{aligned} \quad (5)$$

Fig. 1 Research flow chart



$$\frac{\partial(\rho uv)}{\partial x} + \frac{1}{r} \frac{\partial(r \rho v v)}{\partial r} = -\frac{\partial p}{\partial r} + \frac{\partial}{\partial x} \left[(\mu + \mu_t) \left(\frac{\partial v}{\partial x} + \frac{\partial u}{\partial r} \right) \right] + 2 \frac{1}{r} \frac{\partial}{\partial r} \left[(\mu + \mu_t) r \frac{\partial v}{\partial r} \right] - \frac{2(\mu + \mu_t)v}{r^2} \tag{6}$$

Energy equation:

$$\frac{\partial(\mu T)}{\partial x} + \frac{1}{r} \frac{\partial(r \mu T)}{\partial r} = -\frac{1}{\rho} \frac{\partial}{\partial x} \left[\left(\frac{\mu}{Pr} + \frac{\mu_t}{\sigma_t} \right) \frac{\partial T}{\partial x} \right] + \frac{1}{\rho r} \frac{\partial}{\partial r} \left[\left(\frac{\mu}{Pr} + \frac{\mu_t}{\sigma_t} \right) r \frac{\partial T}{\partial r} \right] \tag{7}$$

Realizable *k*-*ε* equations:

$$\frac{\partial(\mu k)}{\partial x} + \frac{1}{r} \frac{\partial(r \mu k)}{\partial r} = \frac{1}{\rho} \frac{\partial}{\partial x} \left[\left(\mu + \frac{\mu_t}{\sigma_k} \right) \frac{\partial k}{\partial x} \right] + \frac{1}{\rho r} \frac{\partial}{\partial r} \left[\left(\mu + \frac{\mu_t}{\sigma_t} \right) r \frac{\partial k}{\partial r} \right] + G_k + G_b + \epsilon \tag{8}$$

$$\frac{\partial(\mu \epsilon)}{\partial x} + \frac{1}{r} \frac{\partial(r \mu \epsilon)}{\partial r} = \frac{1}{\rho} \frac{\partial}{\partial x} \left[\left(\mu + \frac{\mu_t}{\sigma_\epsilon} \right) \frac{\partial \epsilon}{\partial x} \right] + \frac{1}{\rho r} \frac{\partial}{\partial r} \left[\left(\mu + \frac{\mu_t}{\sigma_\epsilon} \right) r \frac{\partial \epsilon}{\partial r} \right] + C_1 S_\epsilon + C_2 \frac{\epsilon^2}{k + \sqrt{\nu \epsilon}} \tag{9}$$

The Boussinesq approximation was used to model the buoyancy in the SC. The air density in the governing equations was constant during the computation while the body force was replaced by

$$(\rho - \rho_0)g = -\rho_0 \beta (T - T_0)g \tag{10}$$

where T_0 is the reference buoyancy reference temperature and $\beta = 1/T_0$ is the thermal expansion. The ambient air density is 1.20 kg/m^3 , and the expansion rate is 3.31×10^{-3} ,

whereas the air density in other terms was identical to the ambient air density throughout the flow domain. The meshing procedure was carried out by ICEM CFD, and the structured (quadrilateral) grid was built throughout the 2D flow main. The flow is three-dimensional, stationary, and turbulent. Because the Rayleigh number of the flow inside the solar chimney power plant (SCPP) was greater than 10^9 , it was turbulent (Ming et al. 2013). To make the computation easier, the STPPs' 3D structure was reduced to a 2D asymmetric form by using the chimney's centerline as the symmetry axis. The meshing procedure was carried out by ICEM CFD, and the structured (quadrilateral) grid was built throughout the 2D flow main, maintaining a y^+ value of 1 with an expansion ratio of 1.2. The length of the element edge varied from 0. m to 0.55 m. The near-wall region had a 10-boundary layer grid for dealing with the fast changes within the near-wall region. A heat source was added within a thin layer below the ground surface for modeling the heat transfer between the ground and the working air. The heat generation rate was set to 7200 kW/m^3 by assuming solar insolation of 1000 W/m^2 and the transmissivity of the roof and absorption of the ground to be 0.9 and 0.8, respectively, and the solar insolation was handled as a heat source within a thin layer below the ground surface. The adiabaticity of the remaining solid borders is assumed. The second-order upwind schemes are used to discretize the governing equations and solved by the SIMPLE algorithm in the

Table 1 Boundary conditions

Location	Type	Description
Collector	Wall	Mixed, semi-transparent
Ground or base	Wall	Coupled; $Q = q \cdot \alpha \cdot \beta$; $D = 0.0001$ m solar load model
Tower wall	Wall	$q = 0$ W/m ²
Collector inlet	Pressure inlet	$P_{\text{gauge}} = 0$ Pa
Tower outlet	Pressure outlet	$P_{\text{gauge}} = 0$ Pa

commercial CFD software ANSYS with the corresponding boundary conditions mentioned above (Table 1).

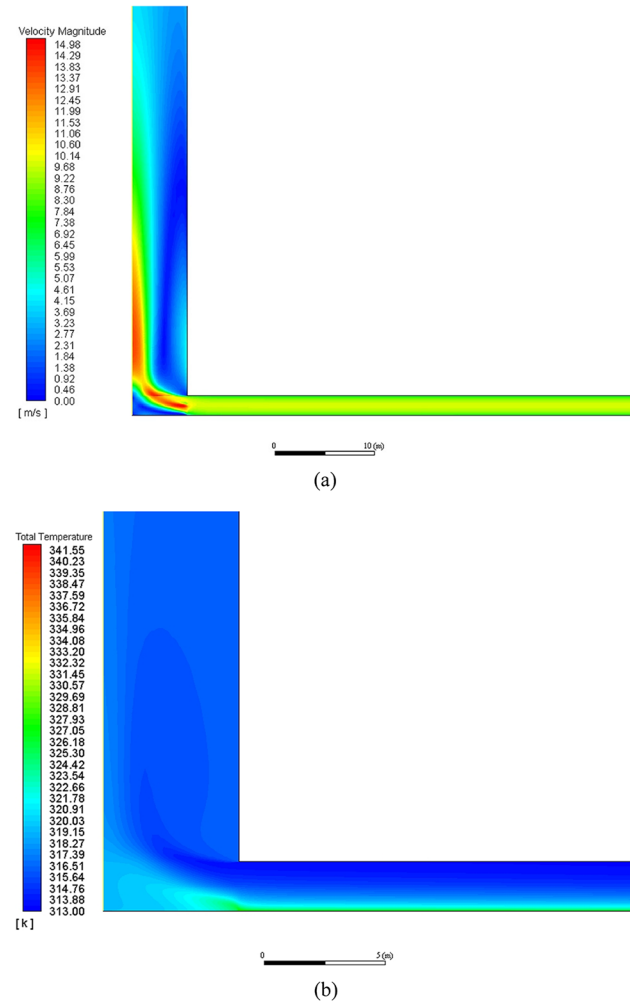


Fig. 2 a Velocity contour of the Manzanares Spanish plant. b Temperature contour of the Manzanares Spanish plant

Table 2 Comparisons of the CFD result with literature

Results	Temperature rise (K)	Velocity (m/s)
Manzanares [1]	20	15
This work (simulation)	23.59	13.67
Lim Beng Hooi [15] (simulation)	21.9	15.7

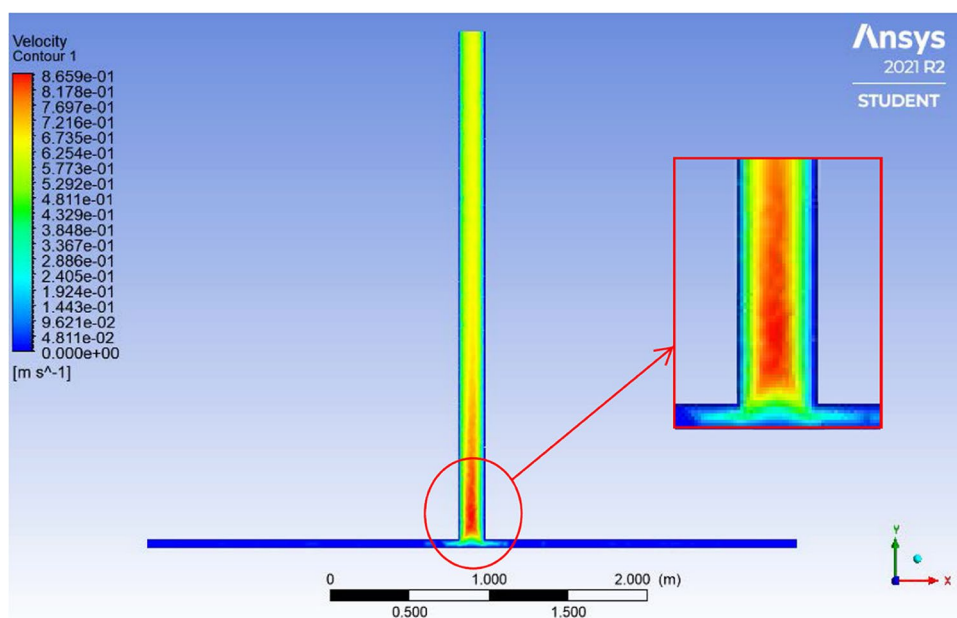
Validation of simulation results

The CFD model is validated through the temperature rises in the collector, and the updraft velocity at the tower inlet, and compared with literature (Beng 2018). The Manzanares prototype experimental results indicate that, when the solar radiation is 1000 W/m², the upwind velocity at the tower base is 15 m/s and the temperature increase through the collector beneath no-load conditions reaches 20 K. The temperature and velocity of the simulated Manzanares plant are shown in Fig. 2a and b, respectively. And the comparison of the reported and simulated results is shown in Table 2. Through Table 2, good quantitative agreement is observed between the Manzanares plant and the CFD results. Thus, the CFD methodology is followed for all models.



Fig. 3 Experimental setup of exp. 1

Fig. 4 Velocity contour of model 1 (1:62)



Experimental studies

Three STPPs, one with a flat collector cum straight diffuser the same as that of the Manzanares plant (model 1), the second one with an inclined collector with a partially divergent tower (model 2), and the third being the fully divergent tower with a semi-convergent collector (model 3) adopted to Manzanares plant, are designed, fabricated, and experimented. For all studies, the Manzanares plant is kept as a reference model. The tower is made up of a 5-inch polyvinyl pipe with a 1.5-m radius, the collector is transparently made

of a 250- μm polythene cover, and the divergent section from the tower to the collector is of sheet metal. The entire structure rests on the steel bars. The connecting rods are attached to the tower by nut and bolt arrangement. These rods form the platform over which the polyethylene sheets are spread. The aluminum sheet is attached, and the divergent portions are also attached

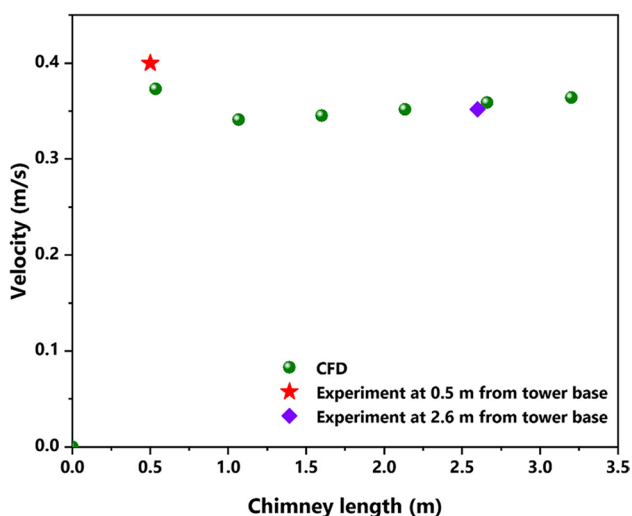


Fig. 5 Computational and experimental validation of model 1 (1:62)

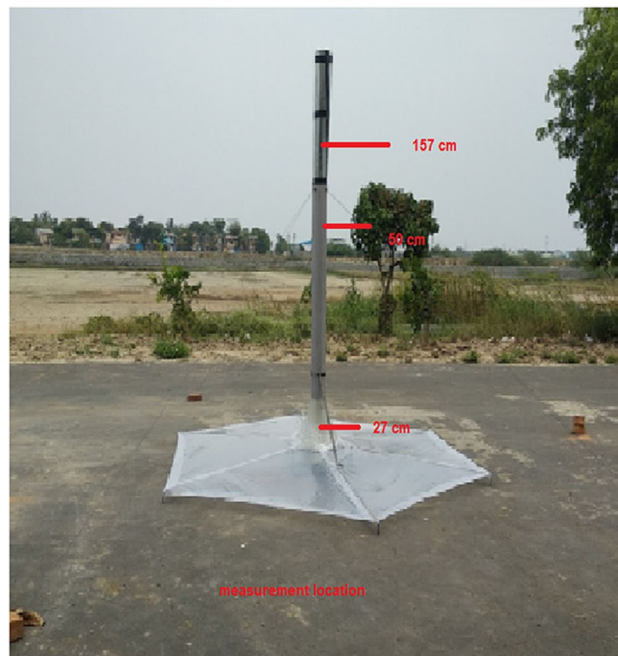
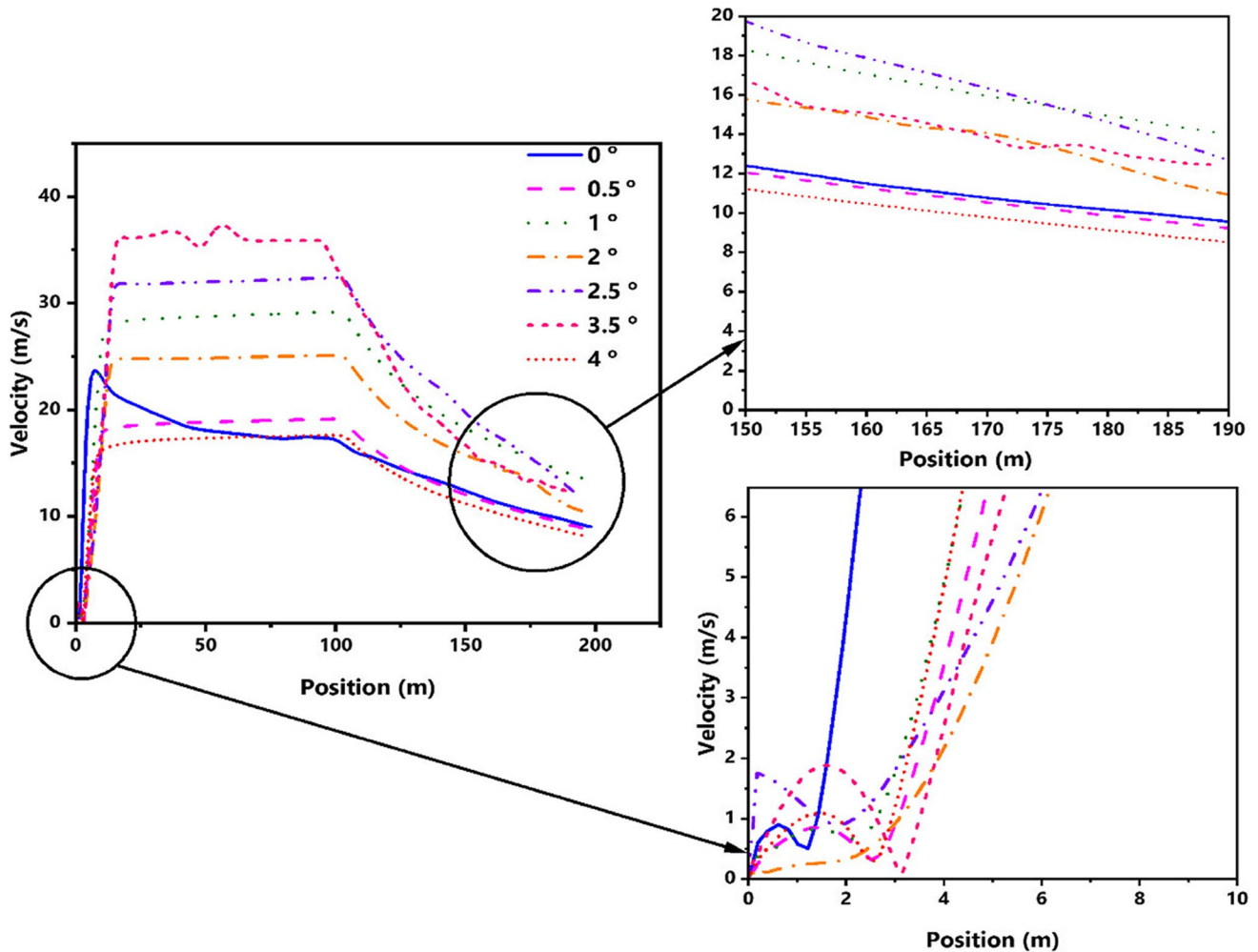


Fig. 6 Experimental setup of exp. 2

Table 3 Comparison of original and scaled dimension

Parts	Spanish plant	Exp. 1 (1:62)	Exp. 2 (1:70)	Exp. 3 (1:122)
Tower height, H_{chim}	198 m	4.1 m	2.4 m	2 m
Tower entry radius, R_{entry}	2 m	0.1655 m	0.073 m	0.08 m
Tower exit radius, R_{exit}	5.09 m	0.1655 m	0.0855 m	0.20 m
Collector radius, R_{coll}	122 m	2.05 m	1.5 m	1.88 m
Collector height	1.85 m	0.0264 m	0.0264 m	0.2 m
Collector angle	3.5°	00	3.5°	0.50

**Fig. 7** Velocity variation along chimney length of semi-divergent chimney with inclined collector model

with the PVC pipe and are attached to the rest of the setup. Now the polyethylene sheets that are mainly used for radiation effects are placed over the supporting rods; a solar collector made up of a polycarbonate transparent sheet which is readily available in the market has been placed over the wooden frames. The collector inclination is achieved by varying the inlet and outlet height. The diameter of the collector is its height from the ground; the ground is chosen as a

cement concrete floor. The tower is made up of thin GI sheets of millimeter thickness; by placing the inner brace wheels for structural stiffness, it is held vertically upwards over a base made up of a thick iron bell-mouthed frame. The entire structure is tightly held by steel wires. The hot wire anemometer measures temperature of accuracy range from ± 3 to $\pm 0.1\%$ and also measures velocity ranging from 0.0 to 30.0 m/s with a resolution of 0.001.

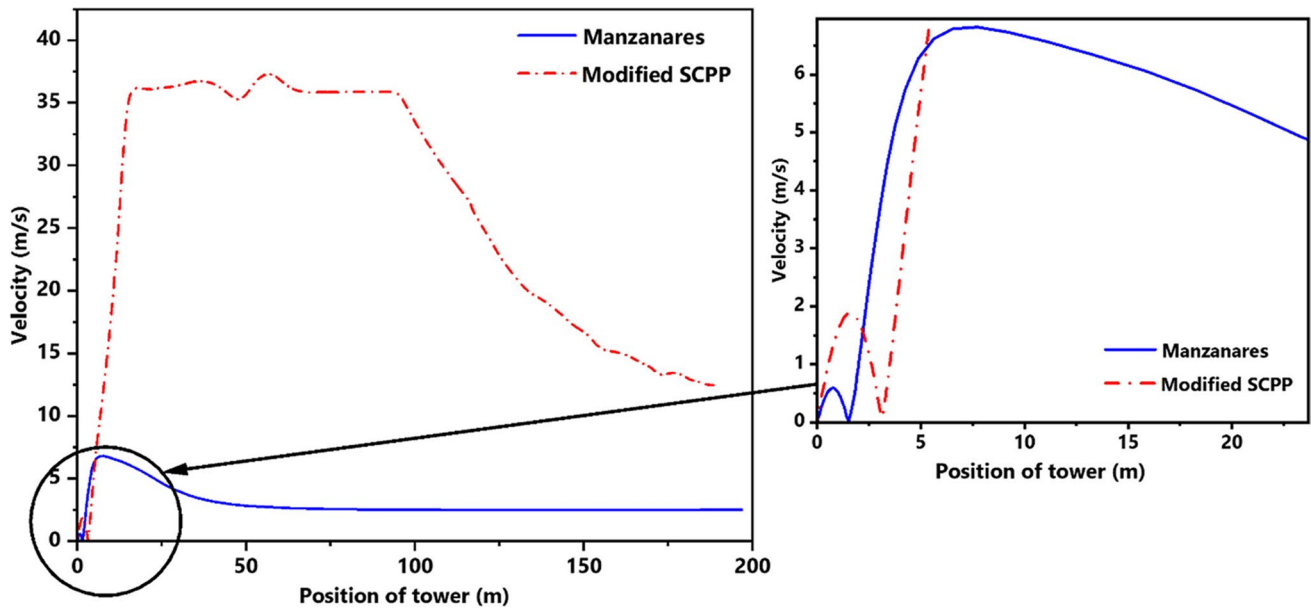


Fig. 8 Comparison of velocities at the tower entrance (base) for exp. 1 and exp. 2

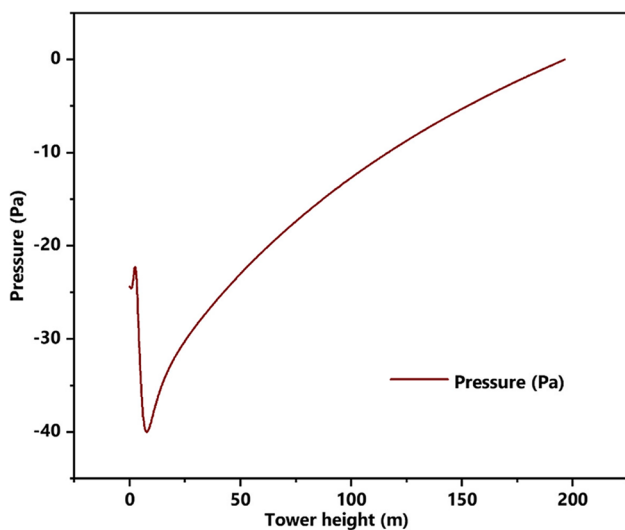


Fig. 9 Tower height vs static pressure for exp. model 2 (original scale)

Investigation of flat collector solar tower (model 1)

The solar tower is built with a scale ratio (in two similar geometric figures, the ratio of their corresponding sides is called the scale ratio) of 1:62 and tested on a tar-based surface from 10 a.m. to 3 p.m. for 5 days. The outside ambient temperature T_0 and the air velocity were measured by a hot wire anemometer. The temperature at the tower entrance T_i was measured at the same time by an anemometer. The air velocity at different positions 0.02 m from a collector, 0.2 m from the tower base, and 2.6 m from the tower base was

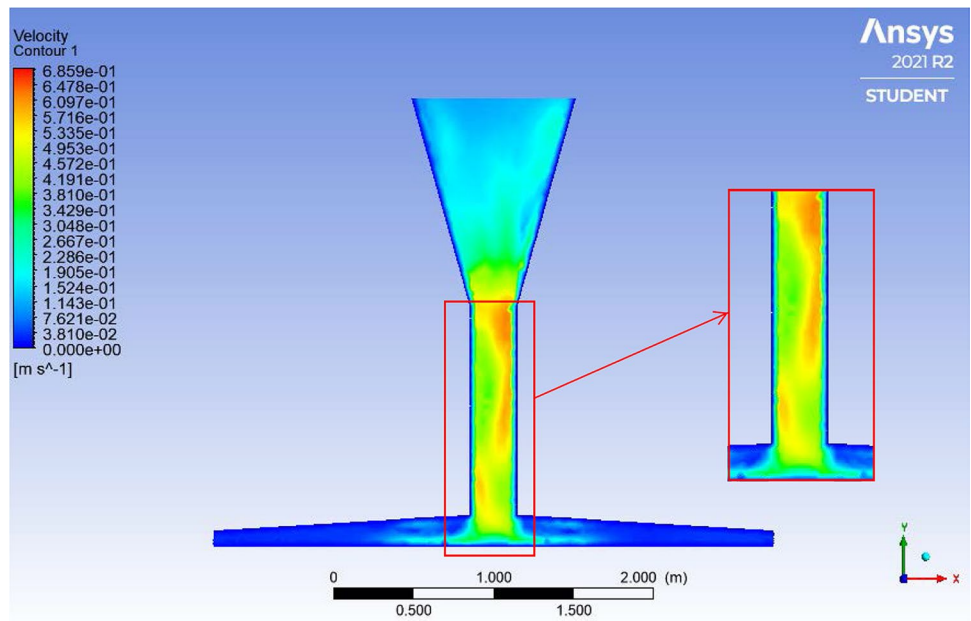
taken (Fig. 3). Theoretically, the plant was designed with the following specifications considering the solar intensity for a normal day was assumed as 1000 W/m^2 ; $\rho_{\text{atm}} = 1.165 \text{ kg/m}^3$ and $\rho_{\text{tower}} = 1.148 \text{ kg/m}^3$ with a power output of 6.98 W. The experiment is validated through simulation studies and found to be in a good match as shown in Figs. 4 and 5.

Investigation of inclined collector solar tower (model 2)

This solar tower is built with a scale ratio of 1:70 and tested as per the method described above. Here the cylindrical tower of the prototype is modified near the collector–tower junction and the exit of the tower is also modified as per the dimensions in Table 3. Model 2 is designed with a collector angle of 3.5° and with an aspect ratio (radius of a tower at the base to the radius at the apex of the tower) as that shown in Fig. 6. The collector slope is decided based on the CFD study by increasing the angle from 0 to 4° . In this work, a numerical investigation was carried out for the proposed diffuser-type solar towers by Hu et al. (2017) incorporating a 3.5° slope in the collector instead of a flat collector. The CFD studies reveal that partially divergent tower is efficient in terms of achieving the maximum velocity of m/s at 2.5 m from the collector base than exp. 1.

The diffuser open angle is at 2° based on the computational results. In the modified shape with a slope in the collector, it is evident from the analysis that for a collector angle of 3.5° , the velocity at the collector outlet is maximum and drops down with a further increment in slope angle. This plant is designed for a power output greater than 6.98 kW.

Fig. 10 Velocity contour for experimental model (1:70)



The general performance of the divergent STPPs is analyzed, and the outcomes from the divergent STPPs are compared with that of the Manzanares pilot plant. The divergent tower height is kept at 198 m, similar to the Manzanares plant. Modifications to the collector have been carried out by replacing the flat collector with an inclined collector with seven varied angles (0.5°, 1°, 2°, 2.5°, 3.5°, and 4°). The CFD analysis indicates that the divergent tower has achieved the maximum velocity of 35.6 m/s for a 3.5° collector as shown in Fig. 7. As the collector inclination angle increases, the mass flow rate increases and hence the velocity increases with minimum pressure loss as shown in Fig. 8, where the

flow velocity along with the tower for both exp. 1 and exp. 2 is compared. The computational results for experimental model 2 (where the scale ratio is 1:70) have proven the fact that the divergent tower with the inclined collector leads to maximum suction effect as shown in Fig. 9. The velocity measured at the tower base showed a remarkable increase (Fig. 10), hence the higher mass flow rate. The temperature at the center of the collector is recorded. This leads to a higher heating rate of incoming air, achieving higher updraft and also taking up more fresh air into the collector.

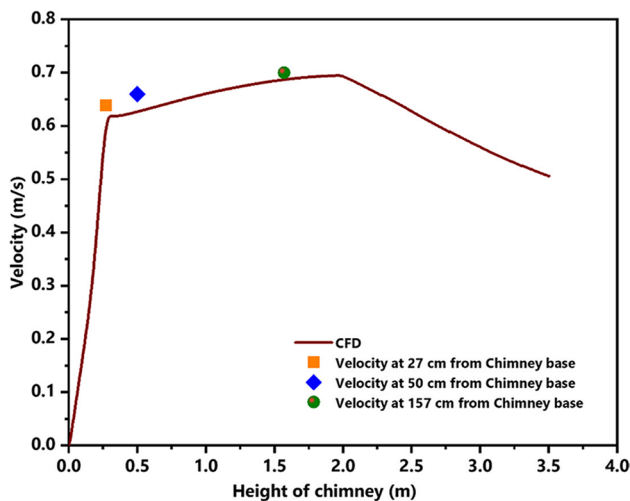


Fig. 11 Comparison of velocity for both experimental and computational model 2 (1:70)

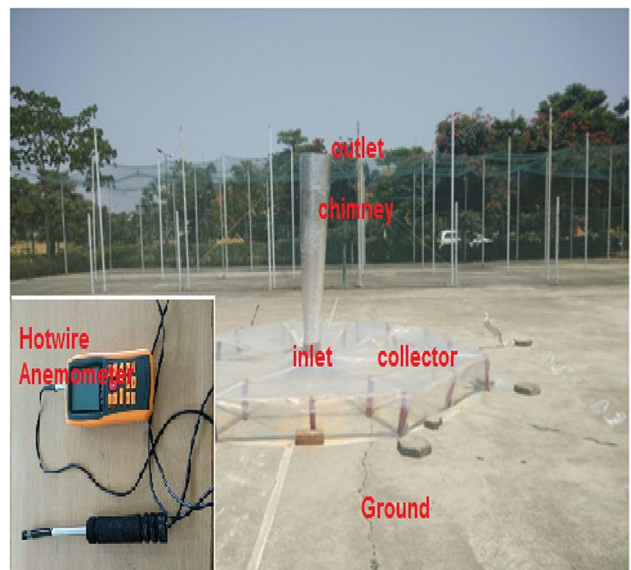
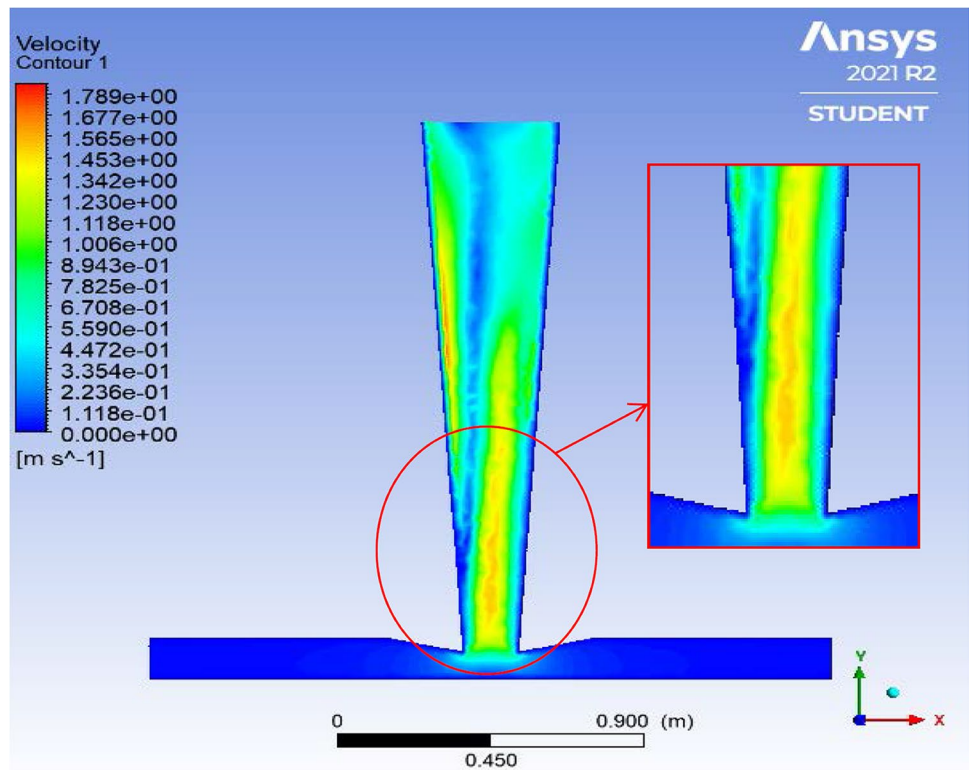


Fig. 12 Experimental setup of exp. 3

Fig. 13 Velocity contour of the experimental model (1:122)



The CFD and experimental results had a good aggregate as shown in Fig. 11; the velocity measured on the tower base on a particular day of the experiment yielded a good agreement with CFD results. Thus, using the divergent tower and convergent collector, there was an increase in velocity. The power output of exp. model 1 is higher than the power output of exp. model 2; because of the sloped collector, the air moves with a higher velocity, and due to the divergent

diffuser, the suction effect increases at the base of the tower, which resembles the operation of a low-speed wind tunnel.

Investigation of velocity variation for different collector configurations adapted to a fully divergent tower.

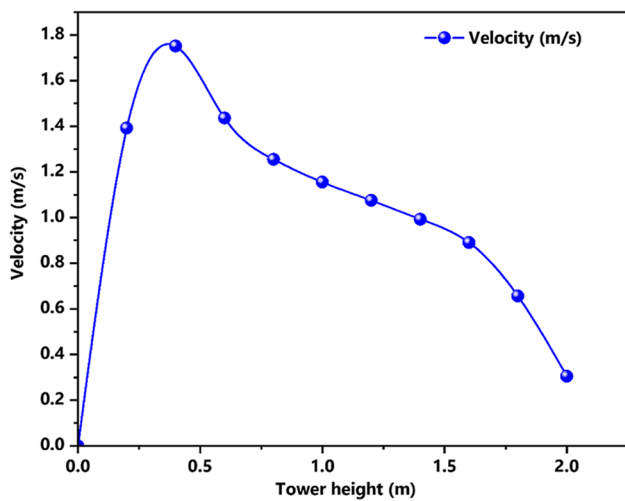


Fig. 14 Velocity variation along the tower length

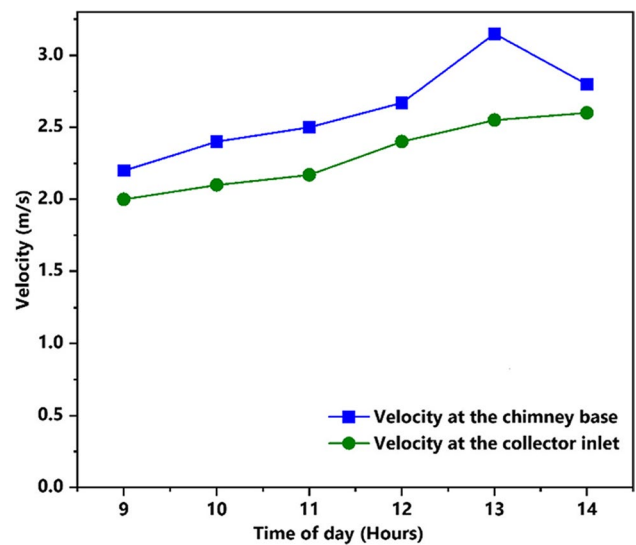


Fig. 15 Velocity variation for experimental model (1:122)

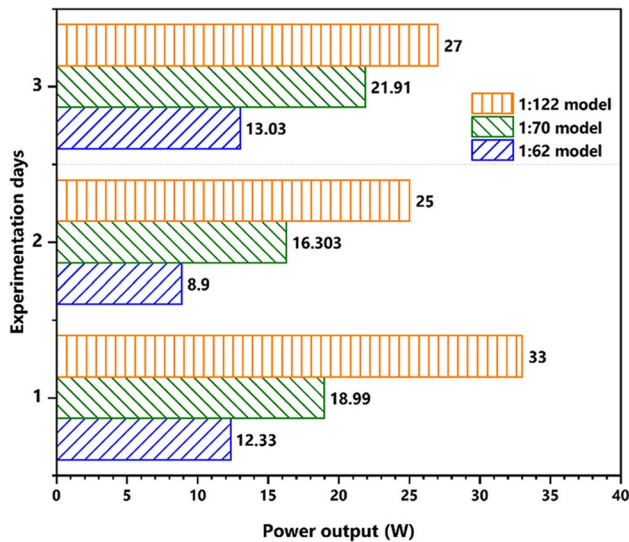


Fig. 16 Comparison of power output for three different configurations

Investigation of divergent tower with a semi-convergent collector (model 3)

The divergent tower with a semi-convergent collector is designed (Hu et al. 2017) in which the divergence angle of the tower from its centerline is identified as 2° . The Spanish prototype has a 195-m-tall tower with a tower and collector radii as 5 m and 122 m, respectively. The collector's inlet height is 1.85 m. For this work, a 1:122 scaled model of a prototype is considered which has a 2-m-tall tower with a semi-open angle of 2° from its centerline (Fig. 12). The collector inlet height and outlet heights are 0.2 m and 0.1 m, respectively. The collector diameter is 1.2 m. The velocity along the tower and collector is plotted for the experimental study shown in Fig. 13; the velocity slowly paces up at the collector–tower junction and gradually loses momentum because of the deceleration of flow in the divergent section.

The velocity of the flow inside the collector initially increases and maintains a constant velocity until 1/3 of its length. In conducting simulation studies for the Spanish prototype, the velocity did not shoot up to near the collector outlet. This indicates the air moves slowly at a constant flow rate, thereby the mass flow increases, but once the area converges, the air rushes into the duct region, thereby the velocity shoots up, which is the notable advantage of this model. The experimental study was carried out from 9 a.m. to 2 p.m. Figure 14 presents the velocity variation along the collector–tower junction. The highest velocity occurs at 1:00 p.m., and for the semi-convergent collector, at 1:00 p.m.; the maximum achieved velocity rises to 3.15 m/s (Fig. 15).

The reduction in the collector area gives a higher airflow velocity. The comparison of these results shows that the collector roof angle has a direct influence on the magnitude velocity of the airflow inside the SCPP. In reality, according to Ayadi et al.'s (2017) research, the negative angle has an effect on the magnitude velocity. This study also supports the findings of Chitsoomban et al. (2014), who found that divergent chimneys outperform conventional cylindrical towers. Due to the significant increment in the velocity and temperature, the divergent tower with a semi-convergent collector enhances the power output by 54% more than the conventional STPP.

For a 3.2-m-tall tower with a 4.1-m collector diameter, experimental model 1 (1:62) yields an average theoretical power output of 13 W with a peak velocity of 0.37 m/s. Furthermore, on a 2.8-m tower with a 3.2-m collector diameter inclined at 3.5° , experimental model 2 (1:70) scaled model of a partially divergent tower with an inclined collector achieved a power output of 21.91 W with a measured peak velocity of 0.68 m/s. An increment in power output by 54% when compared with the previous one is achieved. Experimental model 3 of a 2-m tower with a 2-m semi-convergent collector diameter inclined at 0.33° (1:122) achieves a power output of 33 W with a measured peak velocity of 2.5 m/s, delivering power output thrice that of the 1:62 model as shown in Fig. 16.

Conclusion

To increase the efficiency of the STPP by varying the existing geometry shape is identified as the prime objective of this work. From the literature considering the simulation and experimental studies on SCPP, the base work of the research is attributed to Hu et al. (2017), Patel et al. (2014), and Koonsrisuk et al. (2013). Both computational and experimental methods are studied to assess the aerodynamic performance of solar chimney power plants with variable collector and chimney geometries. The conclusion of the above-discussed results is summarized below.

- It can be concluded from the three different experimental studies that by decreasing the collector reduction area, diffuser-type towers significantly enhance the performance of the solar chimney. In the current study, a fully divergent tower with a semi-convergent collector stood tall among the other experimental models.
- The collector convergence and divergence angle are important parameters in the solar tower design.
- A convergent collector is better than a divergent collector in terms of airflow velocity and temperature.

Acknowledgements The authors extend thanks to the management of Apollo Engineering College, and Sri Venkateswara College of Engineering, India, for providing a place to carry out the experiments.

Author contribution Rajamurugu Natarajan: Conceptualization, experimentation, calibration of instruments, data collection, and original draft preparation.

Venkatesan Jayaraman: Supervision, conceptualization, and validation of CFD results.

Ravishankar Sathyamurthy: Writing—review and editing, software, and validation of experimental results; also carried out the language corrections.

Data availability The datasets used and/or analyzed during the current study are available from the corresponding author on reasonable request.

Declarations

Ethics approval and consent to participate Not applicable.

Consent for publication Not applicable.

Competing interests The authors declare no competing interests.

References

- Ayadi A, Driss Z, Bouabidi A, Abid M (2017) Experimental and numerical study of the impact of the collector roof inclination on the performance of a solar chimney power plant. *Energy Build* 139:263–276
- Beng HL, Thangavelu SK (2018), A parametric simulation of solar chimney power plant, *IOP Conference Series: Mater Sci Eng* p. 297.
- Bernardes MAdS (2010), *Solar chimney power plants - developments and advancements*, Solar Energy, R. D. Rugescu, Ed., ed Croatia, p. 432.
- Cao F, Li H, Guo L, Zhao L (2013) Performance analysis of conventional and sloped solar chimney power plants in China. *Appl Therm Eng* 50:582–592
- Gholamalizadeh E, Kim MH (2016) CFD (computational fluid dynamics) analysis of a solar-chimney power plant with inclined collector roof. *Energy* 107:661–667
- Hu S, Chan JCY, Leung DYC (2017) Numerical modelling and comparison of the performance of diffuser-type solar chimneys for power generation. *Appl Energy* 204:948–957
- Koonsrisuk A (2013) Comparison of conventional solar chimney power plants and sloped solar chimney power plant using second law analysis. *Sol Energy* 98:78–84
- Sakir MT, Khan Piash MB, Akhter MS (2014) Design, construction and performance test of a small solar chimney power plant. *Glob J Res Eng A* 14(1)Version I:21–28
- Morrison RT, Bouabidi A, Abid MS, Ayadi NA, Driss Z (2017) Experimental and numerical study of the impact of the collector roof inclination on the performance of a solar chimney power plant. *Energy Build* 139:263–276
- Rajamurugu N et al. (2021) Experimental and computational studies on performance of a solar chimney power plant with semi convergent collector and divergent chimney *Comptes Rendus De L'académie Bulgare Des Sciences* <https://doi.org/10.7546/CRABS.2020.11.14>
- Rajamurugu N et al. (2021) Experimental and computational flow analysis of geometrically modified solar chimney, *Journal of the Balkan Tribological Association*, Book 1, Vol 26
- Okada S, Karasudani T, Ohya Y, Uchida T (2015) Improvement in solar chimney power generation by using a diffuser tower, *J Solar Energy Eng Trans ASME*, vol. 137, no. 3.
- Patel SK, Ahmed Prasad MR (2014) Computational studies on the effect of geometric parameters on the performance of a SCPP. *Energy Convers Manage* 77:424–431
- Sangi R (2012) Performance evaluation of solar chimney power plants in Iran. *Renew Sustain Energy Rev* 16:704–710
- Schlaich J, Schiel W (2000) *Solar chimneys*, *Encycl Phys Sci Technol* 3rd ed, Elsevier, pp. 1–10

Publisher's note Springer Nature remains neutral with regard to jurisdictional claims in published maps and institutional affiliations.